The Canadian Mineralogist
Vol. 57, pp. 255-265 (2019)
DOI: 10.3749/canmin.1800063

PANDORAITE-Ba AND PANDORAITE-Ca, $Ba(V^{4+}_{5}V^{5+}_{2})O_{16}\cdot 3H_2O$ AND $Ca(V^{4+}_{5}V^{5+}_{2})O_{16}\cdot 3H_2O$, TWO NEW VANADIUM OXIDE BRONZE MINERALS IN SOLID SOLUTION FROM THE PANDORA MINE, LA SAL MINING DISTRICT, SAN JUAN COUNTY, COLORADO, USA

ANTHONY R. KAMPF[§]

Mineral Sciences Department, Natural History Museum of Los Angeles County, 900 Exposition Boulevard, Los Angeles, California 90007, USA

JOHN M. HUGHES

Department of Geology, University of Vermont, Burlington, Vermont 05405, USA

BARBARA P. NASH

Department of Geology and Geophysics, University of Utah, Salt Lake City, Utah 84112, USA

JOE MARTY

5199 East Silver Oak Road, Salt Lake City, Utah 84108, USA

ABSTRACT

Pandoraite-Ba, $BaV^{4+}_{5}V^{5+}_{2}O_{16}\cdot 3H_2O$, and pandoraite-Ca, $CaV^{4+}_{5}V^{5+}_{2}O_{16}\cdot 3H_2O$, are two new vanadium-oxide-bronze minerals from the Pandora mine, La Sal district, San Juan County, Colorado, USA. Pandoraite-Ba and pandoraite-Ca are rare secondary minerals and occur on a matrix consisting of recrystallized quartz grains from the original sandstone. Crystals of carnotite are associated with pandoraite-Ba and crystals of finchite are associated with pandoraite-Ca. The minerals occur as thin, dark blue, square plates up to approximately 100 μm across and approximately 2 μm thick. Plates occur in subparallel to random intergrowths. The streak of both minerals is light greenish blue, and they display a vitreous, transparent luster and brittle tenacity; neither mineral displays fluorescence. The Mohs hardness of pandoraite-Ba and pandoraite-Ca is *ca*. 2½. Cleavage for both minerals is perfect on {001}. For pandoraite-Ba, $density_{meas} = 3.24(1)$ g/cm^3. For pandoraite-Ca, $density_{meas} = 2.91(1)$ g/cm^3. Both minerals are biaxial (pseudo-uniaxial) (–). For pandoraite-Ba, α (ε) =1.81(2), β and γ (ω) = 1.84(1). For pandoraite-Ca, α (ε) = 1.80(2), β and γ (ω) = 1.83(1). Similar greenish-blue pleochroism is found in both minerals, Y and Z (O) > X (E). For pandoraite-Ba, the empirical formula from electron probe microanalysis (EPMA) (calculated on the basis of V + Fe + Al = 7 and O = 19 *apfu*) is $(Ba_{0.83}Sr_{0.09}Ca_{0.05}Na_{0.03}K_{0.02})_{\Sigma 1.02}(V^{4+}_{4.25}V^{5+}_{2.38}Fe^{3+}_{0.35}Al_{0.02})_{\Sigma 7.00}O_{16}\cdot 3H_2O$, and for pandoraite-Ca it is $(Ca_{0.62}Ba_{0.07}Sr_{0.02}Na_{0.01}K_{0.01})_{\Sigma 0.73}(V^{4+}_{3.70}V^{5+}_{2.93}Fe^{3+}_{0.37}Al_{0.01})_{\Sigma 7.01}O_{16}\cdot 3H_2O$. EPMA demonstrates that solid solution exists between the phases. Pandoraite-Ba is monoclinic (pseudo-tetragonal), $P2$, with a 6.1537(16), b 6.1534(18), c 21.356(7) Å, β 90.058(9)°, and V 808.7(4) Å^3, determined by single-crystal X-ray diffractometry. Pandoraite-Ca, inferred to be isostructural with the Ba-dominant phase, has a 6.119(8), b 6.105(8), c 21.460(9)Å, β 90.06(14)°, and V 801.7(15) Å^3, determined by refinement of powder diffraction data. The atomic arrangement of pandoraite-Ba was solved and refined to $R_1 = 0.0573$ for 3652 independent reflections with $I > 2\sigma I$. Pandoraite-Ba and pandoraite-Ca have vanadium oxide bronze layer structures formed of sheets of V_7O_{16} polyhedra that form the structural unit and $(Ba,Ca)(H_2O)_3$ interlayers; the vanadium is of mixed valence (4^+, 5^+), with the reduction of pentavalent vanadium occurring to balance the charge of the Ba "insertion" ions in partially occupied sites in the interlayer. A tetragonal synthetic analog is known.

Keywords: pandoraite-Ca, pandoraite-Ba, new mineral, vanadium oxide bronze, crystal structure, Pandora mine, San Juan County, Colorado, USA.

[§] *Corresponding author e-mail address*: akampf@nhm.org

Introduction and Occurrence

The uranium and vanadium deposits of the Colorado Plateau region of Colorado and Utah have been a rich source of these metals. For over a century, mines have produced the metals from roll-front deposits in sandstone of the Salt Wash member of the Morrison Formation (Carter & Gualtieri 1965, Shawe 2011) in a 120 km long mineralization belt (the Uravan Mineral Belt). The mineralization of U and V took place where solutions rich in the metals encountered locally strongly reducing conditions.

The deposits of the Colorado Plateau and surrounding area have been an unusually rich source of new minerals, particularly vanadium-bearing minerals; 29 minerals with essential vanadium have been described from the Uravan Mineral Belt and nearby areas since 2008. The unique *P-T-X* conditions of mineral genesis in this environment have apparently not been duplicated elsewhere, at least in an environment that has been explored, and the minerals that crystallize under these conditions have extended our knowledge of vanadium minerals greatly. Here we add two additional V-bearing minerals, which occur in solid solution, to the growing list of vanadium-bearing minerals discovered in the uranium-vanadium deposits of the Colorado Plateau.

Pandoraite-Ba and pandoraite-Ca were collected underground at the Pandora mine, La Sal district (Paradox Valley district), San Juan County, Colorado, USA (38.30944, –109.22028). The Pandora mine is located approximately 2.5 km east of La Sal, Utah. The La Sal district does not lie within the nearby Uravan Mineral Belt, which is approximately 30 km to the east; however, the uranium/vanadium mines of the La Sal district occur in a similar geologic setting and have a similar origin. The uranium and vanadium ore mineralization at the Pandora mine was deposited where solutions rich in U and V encountered pockets of strongly reducing solutions that had developed around accumulations of carbonaceous plant material. Mining operations have exposed both unoxidized and oxidized U and V phases. Under ambient temperatures and generally oxidizing near-surface conditions, water reacts with pyrite and chalcopyrite to form aqueous solutions with relatively low pH, which then react with earlier-formed montroseite-corvusite assemblages, resulting in diverse suites of secondary minerals.

Pandoraite-Ba and pandoraite-Ca are rare and occur on matrix consisting of recrystallized quartz grains from the original sandstone that are intermixed with an unknown Fe-V-oxide phase. Well-formed crystals of carnotite, $K_2(UO_2)_2(VO_4)_2{\cdot}3H_2O$, and tiny plates of a Ba-Fe-V-bearing member of the alunite supergroup are intimately associated with pandoraite-Ba (Fig. 1), whereas remarkably large and well-formed crystals of finchite, $Sr(UO_2)_2(V_2O_8){\cdot}5H_2O$, are associated with pandoraite-Ca (Fig. 2). These associations appear to provide a good means for distinguishing the two species. Specimens were collected on August 15, 2012 by a collecting party consisting of three of the authors (ARK, JMH, and JM) as well as Mickey Gunter and John Rakovan.

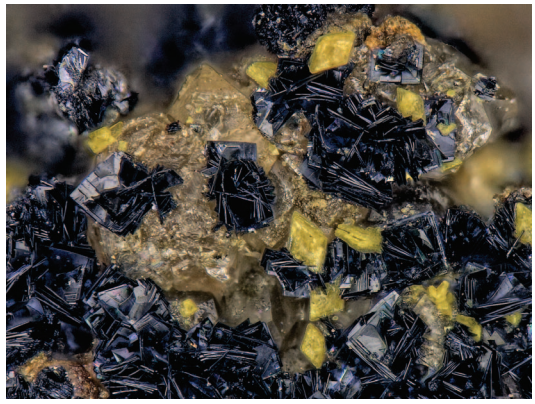

Fig. 1. Pandoraite-Ba plates with yellow carnotite crystals on recrystallized quartz matrix. The field of view is 0.67 mm across.

The mineral names are from the source mine, with the suffix denoting the dominant interlayer cation. The minerals and mineral names, pandoraite-Ba (IMA2018-024) and pandoraite-Ca (2018-036), have been approved by the IMA Commission on New Minerals, Nomenclature and Classification. For pandoraite-Ba, the description is based on two cotype specimens deposited in the collections of the Natural History Museum of Los Angeles County, 900 Exposition Boulevard, Los Angeles, California 90007, USA, under catalogue numbers 67293 and 67294. For pandoraite-Ca, the description is based on one holotype specimen deposited in the same collections under catalogue number 67287.

Appearance and Physical Properties

Pandoraite-Ba and pandoraite-Ca crystals are indistinguishable in hand specimen. The minerals occur as thin, dark blue, square plates up to approximately 100 μm across and approximately 2 μm thick. Plates occur in subparallel to random intergrowths (Figs. 1 and 2). Most of the physical properties of the two species are the same. They have light greenish-blue streak, vitreous luster, brittle tenacity, curved fracture, and perfect cleavage on {001}, Mohs hardness of *ca.* 2½; they are nonfluorescent in both short- and long-wave ultraviolet light. The

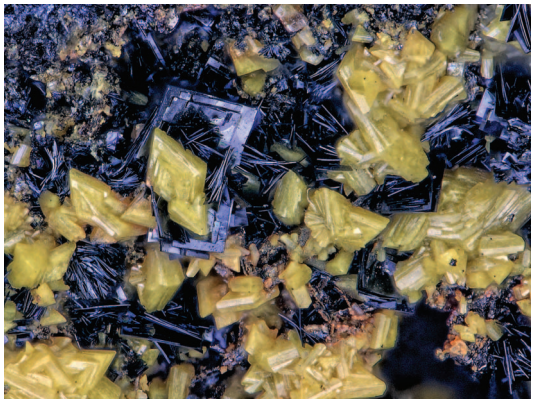

FIG. 2. Pandoraite-Ca plates with yellow finchite crystals on recrystallized quartz matrix. The field of view is 0.84 mm across. Pandoraite-Ba is indistinguishable in hand specimen from pandoraite-Ca.

densities measured by flotation in methylene iodide–toluene are 3.24(1) g/cm^3 for pandoraite-Ba and 2.91(1) g/cm^3 for pandoraite-Ca. The calculated densities for pandoraite-Ba are 3.256 g/cm^3 for the empirical formula and 3.301 g/cm^3 for the ideal formula. Those for pandoraite-Ca are 2.920 g/cm^3 for the empirical formula and 2.927 g/cm^3 for the ideal formula.

For both minerals, the dark color and thinness of the plates made the optical determinations very difficult. Conoscopic observation was not possible, but the optics are expected to be essentially uniaxial. For each mineral, β and γ correspond to ω, and α corresponds to ε; so that their optic signs are negative and $X \approx \mathbf{c}$. Indices of refraction measured in white light for pandoraite-Ba are $\omega = 1.84(1)$, $\varepsilon = 1.81(2)$ and those for pandoraite-Ca are $\omega = 1.83(1)$, $\varepsilon = 1.80(2)$. The larger uncertainty for ε reflects the greater difficulty in observing the Becke line along the edges of the thin plates. The pleochroism in shades of greenish blue is $O > E$.

CHEMICAL COMPOSITIONS

Analyses of pandoraite-Ba (five points on two crystals) and pandoraite-Ca (four points on three crystals) were performed at the University of Utah using a Cameca SX-50 electron microprobe with four wavelength dispersive spectrometers and Probe for EPMA software. Analytical conditions were 15 kV accelerating voltage, 20 nA beam current, and 5 and 10 μm beam diameters. Counting times were 30 s on peak and 30 s on background for each element. Raw X-ray intensities were corrected for matrix effects with a $\phi\rho(z)$ algorithm (Pouchou & Pichoir 1991). No other elements were detected by EDS or by WDS wavescans.

The crystals took a good polish and there was no visible beam damage; however, for pandoraite-Ba, the thinness of the blades made it impossible to avoid including a small amount of epoxy in the analyzed volumes, which accounts for the low analytical total. For both pandoraite phases, insufficient material was available for direct determination of H_2O. Thus, for both minerals, H_2O was calculated based upon the structure determination with (V + Fe + Al) = 7 and O = 19 *apfu*. The results are given in Table 1.

For pandoraite-Ba, the empirical formula is $(Ba_{0.83}Sr_{0.09}Ca_{0.05}Na_{0.03}K_{0.02})_{\Sigma 1.02}(V^{4+}_{4.25}V^{5+}_{2.38}Fe^{3+}_{0.35}Al_{0.02})_{\Sigma 7.00}O_{16}\cdot 3H_2O$. The ideal formula is $BaV^{4+}_5V^{5+}_2O_{16}\cdot 3H_2O$, which requires BaO 19.07, VO_2 51.58, V_2O_5 22.62, and H_2O 6.72, total 99.99 wt.%. For pandoraite-Ca, the empirical formula

TABLE 1A. CHEMICAL COMPOSITION (wt.%) OF PANDORAITE-Ba

Constituent	Mean	Min	Max	S.D.	Standard	Normalized
Na_2O	0.11	0.09	0.13	0.02	albite	0.11
K_2O	0.09	0.09	0.11	0.01	sanidine	0.09
CaO	0.36	0.33	0.44	0.05	diopside	0.37
SrO	1.10	0.87	1.32	0.16	celestine	1.14
BaO	15.54	15.31	15.67	0.17	baryte	16.07
Al_2O_3	0.13	0.10	0.15	0.02	sanidine	0.13
Fe_2O_3	3.41	3.26	3.53	0.11	hematite	3.53
VO_2	(67.07)	66.60	67.69	0.50	V metal	
VO_2*	42.99					44.44
V_2O_5*	26.40					27.29
H_2O†	6.60					6.82
Total	96.73					99.99

* Allocated for charge balance.
† Based on structure with V + Fe + Al = 7 and O = 19 *apfu*.

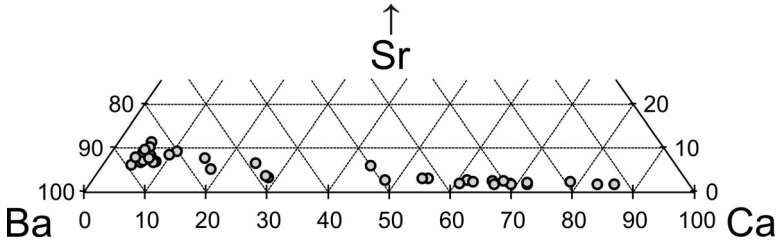

FIG. 3. A portion of the atomic Ba–Ca–Sr ternary illustrating compositional variation in interlayer cation sites for pandoraite-Ca and pandoraite-Ba solid solution, as determined by electron microprobe. Note the increased amounts of substituent Sr in pandoraite-Ba.

calculated on the same formula basis is $(Ca_{0.62}Ba_{0.07}Sr_{0.02}Na_{0.01}K_{0.01})_{\Sigma 0.73}(V^{4+}_{3.70}V^{5+}_{2.93}Fe^{3+}_{0.37}Al_{0.01})_{\Sigma 7.01}O_{16}\cdot 3H_2O$. The ideal formula is $CaV^{4+}_5V^{5+}_2O_{16}\cdot 3H_2O$, which requires CaO 7.94, VO_2 58.68, V_2O_5 25.74, and H_2O 7.65, total 100.01 wt.%. Additional electron microprobe analyses (not reported here) indicate that a complete solid solution exists between pandoraite-Ba and pandoraite-Ca (Fig. 3).

CRYSTAL STRUCTURE EXPERIMENTAL

The X-ray powder diffraction studies were carried out using a Rigaku R-Axis Rapid II curved imaging-plate microdiffractometer with monochromatized Mo$K\alpha$ radiation. A Gandolfi-like motion on the φ and ω axes was used to randomize the samples. Observed *d* values and intensities were derived by profile fitting using JADE 2010 software. Data, including unit-cell parameters refined from the powder data using JADE 2010 with whole pattern fitting, are given in Table 2.

For pandoraite-Ba, intensity data for solution and refinement of the atomic arrangement were collected with a Bruker D8 three-circle diffractometer using a rotating anode generator (Mo$K\alpha$ X-radiation), multilayer optics, and an APEX-II CCD area detector in the Department of Geological Sciences, University of Manitoba (data collection courtesy of Mark Cooper). The complete Ewald sphere of data (including some duplicates) was collected for 38 s per 0.5° frame. The crystal that was utilized in the structure study exhibited weak superlattice reflections that double the final *a* and *b* axes, but those reflections are diffuse streaks along the *c** direction, negating the possibility of collecting data and subsequently solving and refining the atomic arrangement in the quadrupled cell. The data collected in the ultimate $6 \times 6 \times 21$ Å cell suggested an acentric space group, and the pseudo-tetragonal cell metrics yielded one angle that differed significantly from 90° [90.058(9)°]. Intensity data statistics suggested space group *P*2 ($R_{int} = 0.0235$), which was ultimately used to solve and refine the atomic arrangement. Empirical absorption corrections (SADABS; Sheldrick 2015) were applied and equivalent reflections were merged. The structure was solved by direct methods using SHELXS-2013 and the structure was refined using SHELXL-2013

TABLE 1B. CHEMICAL COMPOSITION (wt.%) OF PANDORAITE-Ca

Constituent	Mean	Min	Max	S.D.	Standard
Na_2O	0.06	0.03	0.10	0.03	albite
K_2O	0.08	0.06	0.10	0.02	sanidine
CaO	4.88	4.75	5.06	0.13	diopside
SrO	0.23	0.20	0.29	0.04	celestine
BaO	1.54	1.02	2.14	0.46	baryte
Al_2O_3	0.05	0.03	0.07	0.01	sanidine
Fe_2O_3	4.13	3.94	4.28	0.14	hematite
VO_2	(77.64)	77.17	78.17	0.41	V metal
VO_2*	43.33				
V_2O_5*	37.62				
H_2O†	7.65				
Total	99.57				

* Allocated for charge balance.
† Based on structure with V + Fe + Al = 7 and O = 19 *apfu*.

TABLE 2. POWDER X-RAY DIFFRACTION DATA (*d* IN Å) FOR PANDORAITE-(Ba) AND PANDORAITE-(Ca) COMPARED WITH CALCULATED POWDER X-RAY DIFFRACTION DATA FOR PANDORAITE-(Ba)*

Pandoraite-Ba					Pandoraite-Ca		Pandoraite-Ba					Pandoraite-Ca	
I_{obs}	d_{obs}	d_{calc}	I_{calc}	*h k l*	d_{obs}	I_{obs}	I_{obs}	d_{obs}	d_{calc}	I_{calc}	*h k l*	d_{obs}	I_{obs}
100	10.9	10.6780	100	0 0 2	11.07	100			1.8775	1	$\bar{3}$ 1 3		
9	6.11	6.1534	8	0 1 0	6.14	9	6	1.8116	1.7979	3	$\bar{2}$ 1 9	1.8042	3
		5.9128	2	0 1 1	5.65	5			1.7967	3	1 2 9		
12	5.41	5.3390	7	0 0 4	5.37	9			1.7710	1	$\bar{1}$ 3 5		
		5.3315	2	0 1 2					1.7702	1	3 1 5		
10	4.67	4.6553	7	0 1 3	4.676	8			1.7081	3	$\bar{3}$ 1 6		
6	4.31	4.3512	3	1 1 0	4.355	6	9	1.704	1.7072	5	1 3 6	1.7051	10
10	4.027	4.0305	13	$\bar{1}$ 1 2	4.055	12			1.7012	3	3 2 1		
18	3.631	3.5593	12	0 0 6	3.629	11			1.6879	1	$\bar{2}$ 1 10		
		3.5088	1	0 1 5			5	1.666	1.6871	1	$\bar{2}$ 2 8	1.6770	3
9	3.385	3.3741	6	$\bar{1}$ 1 4	3.399	7			1.6855	3	$\bar{3}$ 2 2		
11	3.112	3.0810	11	0 1 6	3.084	16			1.6599	1	$\bar{2}$ 3 3		
12	3.057	3.0767	7	0 2 0			6	1.6369	1.6413	2	$\bar{3}$ 1 7	1.6559	5
		3.0453	2	0 2 1	2.981	5			1.6404	1	1 3 7		
3	2.947	2.9564	3	0 2 2					1.5867	1	$\bar{1}$ 2 11		
19	2.812	2.8242	15	0 2 3	2.831	14	8	1.5785	1.5857	2	2 1 11	1.5851	3
		2.7560	5	$\bar{1}$ 1 6					1.5727	3	$\bar{1}$ 3 8		
20	2.739	2.7540	4	1 1 6	2.745	22			1.5718	1	3 1 8		
		2.7519	12	1 2 0			5	1.5342	1.5384	2	0 4 0	1.5361	6
		2.7292	5	1 2 1					1.5226	1	0 4 2		
6	2.674	2.6695	3	0 0 8	2.684	7			1.5054	1	$\bar{3}$ 1 9		
		2.6643	5	2 1 2			8	1.5067	1.5044	2	1 3 9	1.5052	4
26	2.559	2.5676	26	$\bar{2}$ 1 3	2.564	23			1.5036	1	0 4 3		
2	2.466	2.4490	2	0 1 8					1.4925	1	4 1 0	1.4890	3
		2.4471	1	$\bar{2}$ 1 4					1.4890	2	$\bar{4}$ 1 1		
2	2.302	2.3143	1	$\bar{2}$ 1 5					1.4781	1	1 $\bar{4}$ $\bar{2}$		
		2.2140	2	0 1 9	2.224	4	6	1.4688	1.4498	1	$\bar{2}$ 0 13		
		2.1756	1	2 2 0					1.4491	1	0 2 13	1.4430	5
13	2.176	2.1664	1	0 2 7	2.166	7	10	1.4341	1.4377	5	3 1 10		
		2.1356	8	0 0 10					1.4371	1	3 3 2		
		2.0512	1	3 0 0					1.4108	2	$\bar{1}$ 2 13	1.4116	4
		2.0425	1	2 1 7					1.4100	2	2 1 13		
		2.0175	4	0 1 10	2.0326	6			1.3999	1	$\bar{3}$ 3 4		
		2.0153	1	$\bar{2}$ 2 4					1.3994	1	3 3 4		
		2.0142	1	2 2 4					1.3780	1	$\bar{2}$ 2 12		
		1.9709	2	0 3 3					1.3769	2	$\bar{4}$ 1 6		
20	1.9345	1.9459	5	1 3 0	1.9401	25	14	1.3656	1.3760	5	4 2 0	1.3799	7
		1.9381	11	$\bar{3}$ 1 1					1.3751	1	$\bar{3}$ 1 11		
		1.9177	2	$\bar{1}$ 1 10					1.3742	1	1 3 11		
10	1.9048	1.9166	2	1 1 10					1.3732	2	$\bar{4}$ 2 1		
		1.9147	4	0 3 4					1.3648	2	$\bar{2}$ 4 2	1.3688	5

* Unit-cell parameters refined from powder data: pandoraite-Ba, $a = 6.127(17)$, $b = 6.124(18)$, $c = 21.78(2)$ Å, $\beta = 90.06(12)°$; $V = 817(3)$ Å^3; pandoraite-Ca, $a = 6.119(8)$, $b = 6.105(8)$, $c = 21.460(9)$ Å, $\beta = 90.06(14)°$; $V = 801.7(15)$ Å^3.

(Sheldrick 2015). During the refinement, twinning was evident, and the twinning matrix $[\bar{1}00/0\bar{1}0/001]$ was included in the refinement, with near-equal components of each twin. Sample data and details of data collection are contained in Table 3, and atomic positions for atoms in pandoraite-Ba are contained in Table 4. Table 5 contains selected bond lengths and bond-valence data for the non-hydrogen cations in pandoraite-Ba.

TABLE 3. DATA COLLECTION AND STRUCTURE REFINEMENT DETAILS FOR PANDORAITE-Ba

Diffractometer	Bruker D8 three-circle; multilayer optics; APEX-II CCD
X-ray radiation / source	Mo$K\alpha$ ($\lambda = 0.71073$ Å) / rotating anode
Temperature	293(2) K
Structural Formula	$BaV_7O_{16}\cdot 3H_2O$
Space group	$P2$
Unit cell dimensions	$a = 6.1537(16)$ Å $b = 6.1534(18)$ Å $c = 21.356(7)$ Å $\beta = 90.058(9)^\circ$
V	808.7(4) Å^3
Z	2
Density (for above formula)	3.277 g/cm^3
Absorption coefficient	6.348 mm^{-1}
F(000)	736
Crystal size	75 × 45 × 3 μm
θ range	2.86 to 27.55°
Index ranges	$-7 \le h \le 7$, $-8 \le k \le 8$, $-27 \le l \le 27$
Reflections collected/unique	7344/3711; $R_{int} = 0.0235$
Reflections with $I > 2\sigma I$	3652
Completeness: $\theta = 27.46^\circ$	99.70%
Refinement method	Full-matrix least-squares on F^2
Parameter/restraints	189/1
GoF	1.097
Final R indices [$I > 2\sigma I$]	$R_1 = 0.0573$, $wR_2 = 0.1455$
R indices (all data)	$R_1 = 0.0586$, $wR_2 = 0.1464$
Largest diff. peak/hole	+1.85/–1.08 e·A^{-3}

$R_{int} = \Sigma|F_o^2 - F_o^2(\text{mean})|/\Sigma[F_o^2]$. GoF $= S = \{\Sigma[w(F_o^2 - F_c^2)^2]/(n-p)\}^{1/2}$. $R_1 = \Sigma||F_o| - |F_c||/\Sigma|F_o|$. $wR_2 = \{\Sigma[w(F_o^2 - F_c^2)^2]/\Sigma[w(F_o^2)^2]\}^{1/2}$; $w = 1/[\sigma^2(F_o^2) + (aP)^2 + bP]$ where a is 0.0497, b is 17.2583 and P is $[2F_c^2 + \text{Max}(F_o^2,0)]/3$.

The ubiquitous occurrence of pandoraite-Ca crystals as subparallel intergrowths of plates made single-crystal X-ray studies impossible. However, the powder X-ray diffraction pattern corresponds closely to that of pandoraite-Ba, with which pandoraite-Ca is deemed isostructural.

Atomic Arrangement of Pandoraite-Ba and Pandoraite-Ca

Oxide bronze compounds are phases composed of an array of polyhedra formed of a transition metal (T), of variable valence and bonding to oxygen, and electropositive metal ions (M) that can be present in the structure in non-stoichiometric amounts. The M ions donate electrons to the (largely) covalent array of TOn polyhedra; these electrons are either localized at specific T sites, producing a semiconducting phase, or delocalized within the TOn array, producing a metallic phase. The reader is referred to Hagenmuller (1973) for an excellent summary of the T = vanadium oxide bronzes, upon which portions of this discussion are based.

Because of the variable oxidation states of the T ions, the amount of the M "insertion" ions in the structure need not be stoichiometric, as one T ion is reduced to maintain charge balance for each charge added by an M ion. Generally, the mean oxidation state of the T ion lies between the highest oxidation value of the transition element (p) and the value ($p - 1$). Oxide bronze phases occur with several transition metals T, including tungsten, molybdenum, niobium, and tantalum. The vanadium oxide bronzes, unlike the bronzes of other transition metals, form a wide variety of structures. This variety is due to the relatively small size and ionic-covalent nature of the vanadium ion as compared to other oxide bronze-forming transition metals. Whereas the larger transition metal ions form a regular covalent network of T–O octahedra, the vanadium octahedra are typically distorted, even to the point of forming five-coordinate trigonal pyramids. This distortion results in complex vanadium bronze structure types and imparts a strong anisotropy to their physical properties.

Hughes & Finger (1983) and Evans & Hughes (1990) linked the literature of oxide bronzes in

TABLE 4. ATOMIC COORDINATES AND EQUIVALENT ISOTROPIC ATOMIC DISPLACEMENT PARAMETERS ($Å^2$) FOR PANDORAITE-Ba. U_{EQ} IS DEFINED AS ONE THIRD OF THE TRACE OF THE ORTHOGONALIZED U_{IJ} TENSOR

	x/*a*	*y*/*b*	*z*/*c*	U_{eq}	Occ.
Ba1	1/2	0.8022(11)	0	0.027(2)	$Ba_{0.300(10)}$
Ba2	1/2	0.6404(12)	0	0.022(3)	$Ba_{0.246(10)}$
Ba3	0.2493(10)	0.5916(10)	0.4965(3)	0.0369(19)	$Ba_{0.267(7)}$
Ba4	0.0821(8)	0.2447(13)	0.5015(4)	0.0301(14)	$Ba_{0.250(5)}$
Ba5	0.145(3)	0.4976(18)	0.9932(5)	0.065(5)	$Ba_{0.177(8)}$
Ba6	0.1535(16)	0.998(2)	0.0026(5)	0.033(3)	$Ba_{0.156(7)}$
V1	0.5108(6)	0.2444(7)	0.25019(11)	0.0086(5)	$V_{1.00}$
V2	0.0857(5)	0.9687(5)	0.31442(19)	0.0104(7)	$V_{1.00}$
V3	0.9402(5)	0.5222(5)	0.31388(19)	0.0125(7)	$V_{1.00}$
V4	0.7867(5)	0.8174(6)	0.18590(17)	0.0114(7)	$V_{1.00}$
V5	0.2381(6)	0.6710(5)	0.18574(19)	0.0125(7)	$V_{1.00}$
V6	0.0097(7)	0.2447(6)	0.18141(12)	0.0114(5)	$V_{1.00}$
V7	0.5125(6)	0.7467(6)	0.31852(13)	0.0108(5)	$V_{1.00}$
O1	0.402(2)	0.045(3)	0.3006(6)	0.012(3)	$O_{1.00}$
O2	0.721(2)	0.133(2)	0.1962(6)	0.014(3)	$O_{1.00}$
O3	0.314(2)	0.360(3)	0.2007(6)	0.011(3)	$O_{1.00}$
O4	0.634(2)	0.444(2)	0.3038(6)	0.011(3)	$O_{1.00}$
O5	0.203(2)	0.664(2)	0.2995(6)	0.005(3)	$O_{1.00}$
O6	0.816(3)	0.813(3)	0.2959(8)	0.023(4)	$O_{1.00}$
O7	0.081(2)	0.944(2)	0.2055(6)	0.010(3)	$O_{1.00}$
O8	0.938(2)	0.553(3)	0.1993(7)	0.019(4)	$O_{1.00}$
O9	0.019(2)	0.249(2)	0.2881(4)	0.008(2)	$O_{1.00}$
O10	0.504(3)	0.742(3)	0.2132(5)	0.015(2)	$O_{1.00}$
O11	0.963(3)	0.503(3)	0.3890(7)	0.020(3)	$O_{1.00}$
O12	0.078(2)	0.997(2)	0.3888(6)	0.014(3)	$O_{1.00}$
O13	0.264(3)	0.678(3)	0.1113(7)	0.019(3)	$O_{1.00}$
O14	0.994(4)	0.243(3)	0.1063(5)	0.024(2)	$O_{1.00}$
O15	0.771(3)	0.795(3)	0.1109(8)	0.024(3)	$O_{1.00}$
O16	0.524(3)	0.747(3)	0.3944(5)	0.022(3)	$O_{1.00}$
OW1	0.463(5)	0.214(4)	0.5732(11)	0.068(7)	$O_{1.00}$
OW2	0.508(6)	0.187(4)	0.9292(11)	0.073(7)	$O_{1.00}$

synthetic chemistry to naturally occurring oxide bronze phases, and the latter authors detailed the extant vanadium oxide bronze minerals and mineral groups at the time of their writing. In the known vanadium oxide bronze minerals, the vanadium is of mixed valence (4^+, 5^+), with the reduction of pentavalent vanadium occurring to balance the charge of "insertion" ions at fully or partially occupied sites in the structure. Among the types of vanadium oxide bronzes that were recognized at that time, no natural compounds with V_7O_{16} layers were known.

Pandoraite-Ba and pandoraite-Ca are the first naturally occurring vanadium oxide bronze layer structures with V_7O_{16} layers. The structure can be viewed as consisting of two distinct parts: (1) the V_7O_{16} layers, which form the structural unit (Fig. 4), and (2) the $(Ba,Ca)(H_2O)_3$ interlayers (Fig. 5).

The vanadium-oxide layers in pandoraite-Ba (and by analogy, pandoraite-Ca) are composed of six distorted VO_6 octahedra and a seventh V-centered polyhedron as a VO_4 tetrahedron; all the V atoms are at general positions. The six octahedra (V2–V7) contain mixed-valence V (Table 5) save for V7, which is entirely V^{4+}. The sheet is formed of a double layer of edge- and corner-shared octahedra (V2–V7). In one layer (orange in Figs. 4 and 5), V2, V3, and V7 form zigzag chains of edge-sharing VO_6 octahedra; those chains are linked laterally to identical chains by corner sharing. The second layer is formed of similar chains of VO_6 octahedra (V4, V5, and V6; gray in Figs. 4 and 5) that are rotated 90° from those in the first layer. The layers are linked by the $V1O_4$ tetrahedra; each tetrahedron shares two apices with the octahedra in one layer and the other two tetrahedra with the second octahedral layer (Fig. 5).

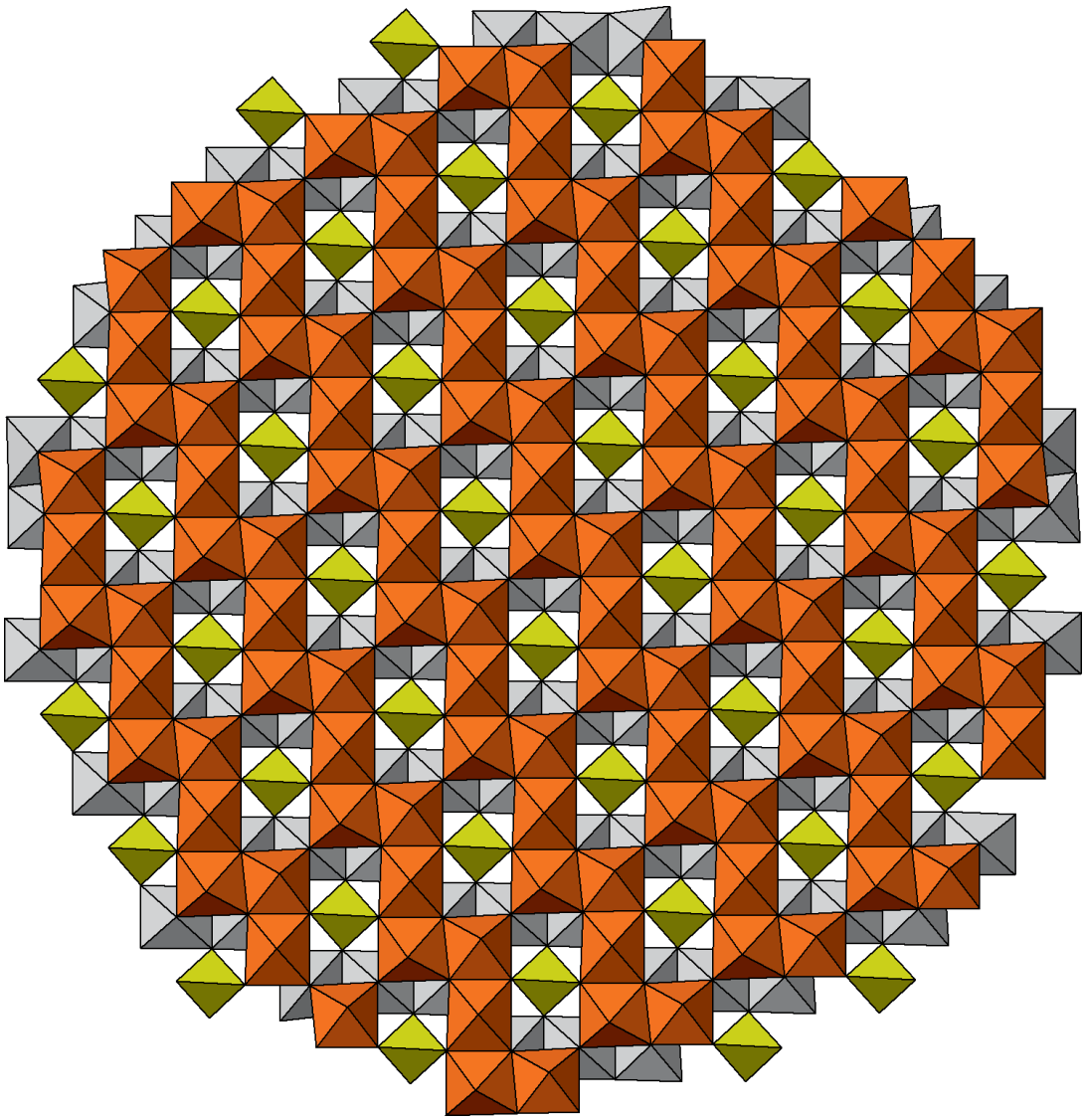

FIG. 4. [001] plan view of V_7O_{16} layers in pandoraite-Ba. The layers are formed of double sheets of chains of edge-sharing VO_6 octahedra; adjacent chains in (001) are linked by corner sharing at "kinks" in the chain (upper sheet in orange, lower sheet in gray). The chains in the two parallel layers are orthogonal to each other (rotated about [001]), and the two sheets that together form the V_7O_{16} layer are linked by corner sharing of the VO_4 tetrahedra (yellow).

In pandoraite-Ba, there are two distinct interlayers (Fig. 5) between the vanadium octahedral layers, in total containing six partially occupied Ba-centered octahedra; the maximum occupancy of any Ba site is 0.300(10) (Table 4). One interlayer contains the Ba1, Ba2, Ba5, and Ba6 sites, each site occurring as a $BaO_4(H_2O)_2$ octahedron with the four bonds to oxygen atoms of the V_7O_{16} layer; two of the oxygen bonds are to the layer above and two to the layer below, linking adjacent V_7O_{16} layers. The Ba sites are too close to have adjacent sites occupied, and thus the partial occupancy of the insertion ion sites results (*cf.* the Na sites in bannermanite; Hughes & Finger 1983). The second interlayer in the unit cell contains the Ba3 and Ba4 sites, also coordinated by $BaO_4(H_2O)_2$ octahedra, and the octahedra also connect the two adjacent interlayers by linking to two oxygen atoms of each adjacent vanadium layer in addition to two H_2O

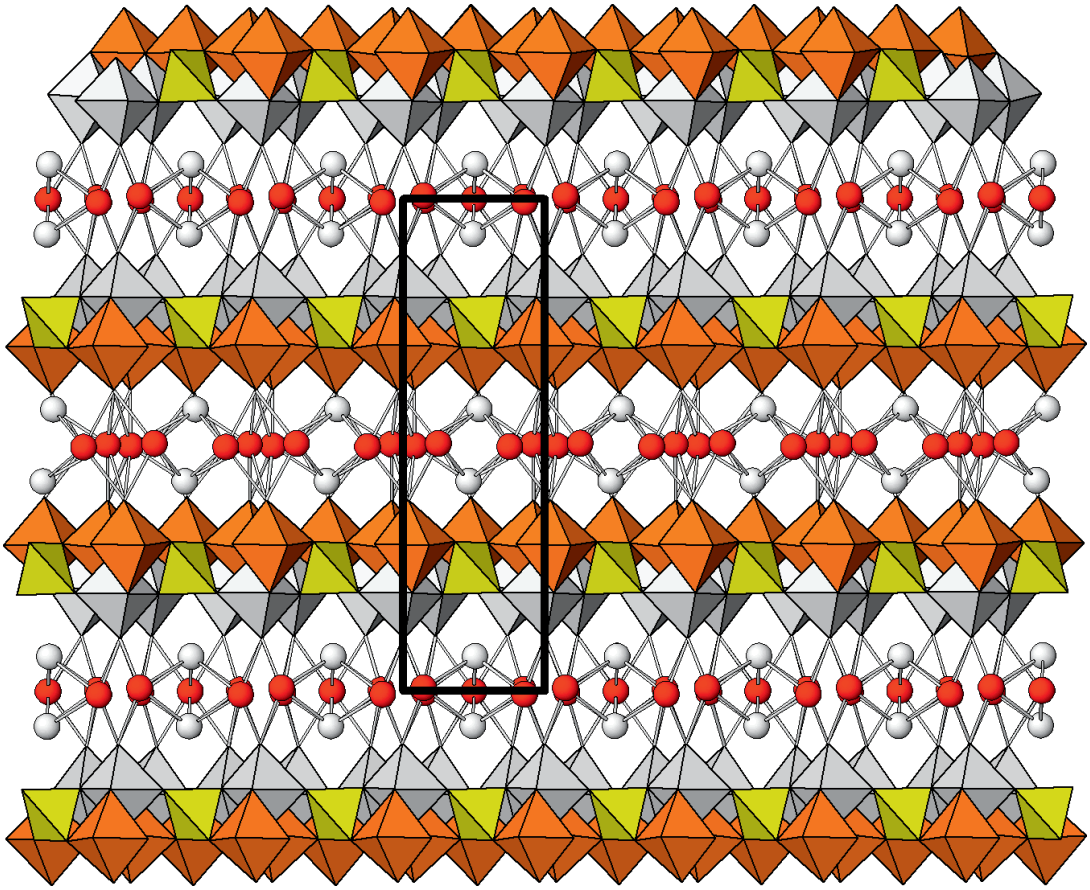

FIG. 5. [010] projection in pandoraite-Ba, with the **c** axis vertical. Partially occupied Ba sites in the interlayer are red and H_2O molecules are gray. The unit cell is outlined. Pandoraite-Ca is isostructural with pandoraite-Ba, with Ca replacing Ba in the interlayers. Colors of layer polyhedra are as in Figure 4.

molecules within the interlayer. The total of the refined Ba occupancies in the interlayers is 1.123 *apfu*, which suggests that a total of approximately one additional H_2O *pfu* also occupies the Ba sites. The total refined site scattering for the Ba sites (1.123 × 56) is 62.9 *e*, which compares reasonably well with the calculated site scattering of 64.0 *e* for 1 Ba and 1 O and 59.6 *e* for $Ba_{0.83}Sr_{0.09}Ca_{0.05}Na_{0.03}K_{0.02}O_{1.00}$, based on the empirical formula.

A similar phase has been previously synthesized. Wang *et al*. (1998) described the atomic arrangement of $BaV_7O_{16}{\cdot}nH_2O$, a tetragonal phase in space group $P4_2/m$, $a = 6.1598(4)$, $c = 21.522(2)$ Å. The pseudo-tetragonal monoclinic cell of pandoraite-Ba compares well with the tetragonal cell of the synthetic phase. The reasons for the reduction in symmetry to monoclinic are not clear. The β value in pandoraite-Ba is 90.058(9)°, and that angle represents the stacking vector of the vanadate layers and intervening interlayers. We can speculate that the difference in crystallization conditions between those in the synthesis and those under natural conditions can cause the minor deviation from orthogonality [0.058(9)°] that results in the dissymmetrization to monoclinic.

As noted above and illustrated in Figure 3, there is a complete solid solution between pandoraite-Ba and pandoraite-Ca, as determined by chemical analysis and by deduction from the powder diffraction patterns and refined unit-cell parameters that the two phases are isostructural.

ACKNOWLEDGMENTS

The manuscript was improved by reviews by Jim Evans and Henrik Friis. Mark Cooper is thanked for the collection of the structure data with the X-ray

TABLE 5. SELECTED BOND LENGTHS (IN Å) AND BOND VALENCES (BV; IN *vu*)* FOR ATOMS IN PANDORAITE-Ba

	Distance	BV		Distance	BV		Distance	BV		Distance	BV
V1–			V2–			V3–			V4–		
O3	1.760(15)	1.07	O12	1.600(14)	1.69	O11	1.615(15)	1.61	O15	1.610(16)	1.64
O1	1.765(16)	1.05	O9	1.861(15)	0.77	O9	1.834(15)	0.83	O10	1.893(21)	0.71
O4	1.843(15)	0.85	O6	1.958(19)	0.59	O5	1.865(14)	0.76	O8	1.896(18)	0.70
O2	1.865(14)	0.80	O1	2.026(15)	0.50	O4	1.953(14)	0.6	O2	1.994(16)	0.54
Mean, sum:	1.808	3.77	O5	2.030(14)	0.49	O6	1.983(20)	0.55	O7	2.014(15)	0.51
			O7	2.330(14)	0.24	O8	2.455(16)	0.18	O6	2.357(17)	0.23
			Mean, sum:	1.968	4.28	Mean, sum:	1.951	4.53	Mean, sum:	1.961	4.33
			Site Valence:	$V^{4+}_{0.72}V^{5+}_{0.28}$		Site Valence:	$V^{4+}_{0.47}V^{5+}_{0.53}$		Site Valence:	$V^{4+}_{0.67}V^{5+}_{0.33}$	
V5–			V6–			V7–			Ba1–		
O13	1.598(15)	1.70	O14	1.607(12)	1.65	O16	1.622(12)	1.57	OW2	2.810(25)	0.24
O10	1.791(21)	0.94	O2	1.931(16)	0.64	O6	1.970(19)	0.57	OW2	2.810(25)	0.24
O7	1.986(15)	0.55	O7	1.969(16)	0.57	O1	1.992(16)	0.54	O13	2.890(16)	0.20
O3	1.994(16)	0.54	O8	1.984(18)	0.55	O5	2.011(14)	0.51	O13	2.890(16)	0.20
O8	2.009(16)	0.52	O3	2.041(16)	0.48	O4	2.032(15)	0.49	O15	2.896(17)	0.19
O5	2.439(13)	0.19	O9	2.279(9)	0.27	O10	2.251(11)	0.29	O15	2.896(17)	0.19
Mean, sum:	1.970	4.44	Mean, sum:	1.969	4.16	Mean, sum:	1.980	3.97	Mean, sum:	2.865	1.26
Site Valence:	$V^{4+}_{0.56}V^{5+}_{0.44}$		Site Valence:	$V^{4+}_{0.84}V^{5+}_{0.16}$		Site Valence:	$V^{4+}_{1.00}V^{5+}_{0.00}$				
Ba2–			Ba3–			Ba4–			Ba5–		
O13	2.796(16)	0.25	O11	2.826(16)	0.23	OW1	2.803(30)	0.25	O14	2.774(21)	0.27
O13	2.796(16)	0.25	O16	2.877(16)	0.20	O11	2.839(18)	0.22	O13	2.850(20)	0.22
O15	3.047(17)	0.13	O16	2.922(16)	0.18	O12	2.849(17)	0.22	O15	2.925(22)	0.18
O15	3.047(17)	0.13	O11	2.945(17)	0.17	O12	2.964(16)	0.16	O14	3.025(20)	0.14
OW2	3.174(25)	0.09	OW1	3.129(28)	0.10	O11	2.972(18)	0.16	OW2	3.245(35)	0.08
OW2	3.174(25)	0.09	OW1	3.280(27)	0.07	OW1	3.232(20)	0.08	OW2	3.311(33)	0.06
Mean, sum:	3.006	0.94	Mean, sum:	2.997	0.95	Mean, sum:	2.943	1.09	Mean, sum:	3.022	0.95
Ba6–											
O15	2.769(21)	0.27									
OW2	2.794(34)	0.26									
O14	2.853(20)	0.22									
O14	2.916(21)	0.18									
OW2	2.929(34)	0.18									
O13	3.119(20)	0.11									
Mean, sum:	2.897	1.22									

Average vanadium valence, V2–V7: $V^{4+}_{0.71}V^{5+}_{0.29}$.

* For V1, constants for V^{4+} and Ba from Brese & O'Keeffe (1991); for V2–V7, mixed-valence V^{4+}/V^{5+} constants from Brown (1981).

diffractometer at the University of Manitoba. This study was funded, in part, by the John Jago Trelawney Endowment to the Mineral Sciences Department of the Natural History Museum of Los Angeles County and by grant NSF-MRI 1039436 from the National Science Foundation to JMH. BPN thanks the Northern California Mineralogical Association for partial support for electron microprobe analyses of new minerals from the Colorado Plateau. We would like to thank Don Coram, the owner of the mine, for allowing us access to the property, and Okie Howell and Jess Fulbright for providing logistical support during our visit.

References

Brese, N.E. & O'Keeffe, M. (1991) Bond valence parameters for solids. *Acta Crystallographica* **B47**, 192–197.

Brown, I.D. (1981) *Structure and Bonding in Crystals*, Volume 2 (M. O'Keefee & A. Navrotsky, eds.). Academic Press, New York City, New York (1–30).

Carter, W.D. & Gualtieri, J.L. (1965) Geology and uranium–vanadium deposits of the La Sal quadrangle, San Juan County, Utah, and Montrose County, Colorado. *United States Geological Survey Professional Paper* **508**.

Evans, H.T., Jr. & Hughes, J.M. (1990) The crystal chemistry of the natural vanadium bronzes. *American Mineralogist* **75**, 508–521.

Hagenmuller, P. (1973) Tungsten bronzes, vanadium bronzes and related compounds. *In* Comprehensive Inorganic Chemistry, Volume 4 (A.F. Trotman-Dickinson, ed.). Pergamon Press, Oxford, England (541 pp.).

Hughes, J.M. & Finger, L.W. (1983) Bannermanite, a new sodium-potassium vanadate isostructural with β-$Na_xV_6O_{15}$. *American Mineralogist* **68**, 634–641.

Pouchou, J.-L. & Pichoir, F. (1991) Quantitative analysis of homogeneous or stratified microvolumes applying the model "PAP". *In* Electron Probe Quantitation (K.F.J. Heinrich & D.E. Newbury, eds.). Plenum Press, New York City, New York (31–75).

Shawe, D.R. (2011) Uranium-vanadium deposits of the Slick Rock district, Colorado. *United States Geological Survey Professional Paper* **576-F**.

Sheldrick, G.M. (2015) Crystal Structure refinement with *SHELX*. *Acta Crystallographica* **C71**, 3–8.

Wang, X., Liu, L., Bontchev, R., & Jacobson, A.J. (1998) Electrochemical-hydrothermal synthesis and structure determination of a novel layered mixed-valence oxide: $BaV_7O_{16}{\cdot}nH_2O$. *Chemical Communications* **1998**, 1009–1010.

Received October 21, 2018. Revised manuscript accepted January 25, 2019.